(Scheme III). Saponification (KOH, EtOH, H_2O), reduction (baker's yeast, D-glucose, H_2O, 25 °C, 2 days), and methylation (CH_2N_2) produced chiral β-hydroxy ester **14**, 35% yield, in >99% ee as determined by ^1H NMR chiral shift studies [360 MHz, $Eu(tfc)_3$]. The absolute configuration was tentatively assigned by analogy to the reduction of 3-oxohexanoate[15a] and confirmed by eventual conversion to natural product **1a** (vide infra). This ester **14**, after conversion to its THP ether, was reduced with DIBAL-H to afford the aldehyde **15** in 85% yield. Transformation of **15** to a chromatographically readily separable 1:1 mixture of **16**[17] and its 3-*R* isomer was performed in a straightforward manner in five steps (48% overall): (i) aldol condensation (EtOAc, LDA, −78 °C), (ii) deprotection of THP ether (PPTS, EtOH), (iii) acetonide formation (2,2-dimethoxypropane, *p*-TsOH), (iv) reduction ($LiAlH_4$), and (v) protection ($PhCH_2Br$, NaH, DMF). Finally, careful ozonolysis of **16** (MeOH, −78 °C → Me_2S) completed the preparation of segment B (**6**) in 88% yield.

The coupling of **5** and **6** in THF (1.3 equiv of NaH, 1.0 equiv of **6**, 0 °C, 5 min → 25 °C, 10 min) smoothly produced the (*E,E,E*)-trienone **4**, 86% yield. Cyclization of **4** in refluxing chlorobenzene (N_2, 82 h) proceeded more slowly than **7** to give the desired *trans*-octalone **3** (28%) and two cis isomers (45% and 9%).[18] The stereochemistry on the octalone ring of **3**, which embodies five correct asymmetric centers out of six in the carbon framework of **1a**, was evident from its ^1H NMR spectrum.[18] K-Selectride reduction (2 equiv in THF, 25 °C) of **3** introduced selectively the requisite axial alcohol **17** (87%).[19] Esterification with 2(*S*)-methylbutyric anhydride (DMAP, pyridine, 25 °C, 20 h) yielded **18** (70%),[19,20] which was debenzylated (Li/NH_3, −78 °C, 10 min; 73%) and oxidized [Collins, PDC(DMF), and CH_2N_2] to the methyl ester **19** (65%). Exposure of **19** to 47% aqueous $HF-CH_3CN$ (1:10) at 25 °C for 1 h resulted in desilylation, deprotection of the acetonide, and subsequent lactonization to afford **20**, mp 178–180 °C, 70% yield. The final operation remaining for the completion of the synthesis, regioselective dehydration of the C13 axial OH in **20**, was initiated by selective protection of the lactonic OH as the *tert*-butyldimethylsilyl ether **21** (65%). Dehydration under the mild condition ($SOCl_2$, pyridine; 0 °C, 15 min → 25 °C, 15 min) followed by removal of the silyl protecting group [47% aqueous $HF-CH_3CN$ (1:10), 25 °C, 30 min] completed the synthesis of **1a** (51% from **21**), which was identical (mp, 360-MHz NMR, IR, UV, MS, $[\alpha]_D$, TLC) with natural ML-236B (compactin).

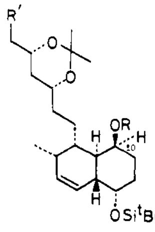

17, R = H; R' = CH_2OBzl
18, R = COCH(Me)Et; R' = CH_2OBzl
19, R = COCH(Me)Et; R' = CO_2Me

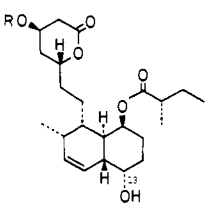

20, R = H
21, R = Si-*t*-BuMe$_2$

Application of the described methodology to the synthesis of analogues and refinement of stereoselectivity are currently under investigation.

Acknowledgment. We thank Professor Akira Endo, Tokyo Noko University, for a generous sample of ML-236B and Drs. Takeo Sakan, Koji Nakanishi, and Kyosuke Nomoto for valuable discussions.

Registry No. 1a, 73573-88-3; **3**, 82080-53-3; **4**, 82080-54-4; **5**, 82065-57-4; **6**, 82065-58-5; **7**, 82080-55-5; **8**, 82065-59-6; **9**, 82065-60-9; **10**, 82065-61-0; **11**, 82065-62-1; **12**, 82065-63-2; **13**, 17605-06-0; **14**, 82065-64-3; **15**, 82065-65-4; **16**, 82065-66-5; **17**, 82065-67-6; **18**, 82065-68-7; **18** debenzylated derivative, 82065-69-8; **19**, 82065-70-1; **20**, 82065-71-2; **21**, 82080-56-6; **16**, 3(*R*) isomer, 82110-38-1; 2(*S*)-methylbutyric anhydride, 65527-79-9; *trans*-crotyl phenyl sulfone, 72863-24-2; *trans*-2-buten-1-ol, 504-61-0; 5-hexen-2-one, 109-49-9.

Supplementary Material Available: Spectroscopic data (NMR and IR) for new compounds described in this paper (27 pages). Ordering information is given on any current masthead page.

---

(17) The desired stereochemistry of **16** was evident from ^1H NMR data: $H_{4\alpha}$ (δ 1.15) appeared as doublet of triplet ($J_{4\alpha,4\beta}$ = 12.7 Hz, $J_{4\alpha,3}$ = $J_{4\alpha,5}$ = 11.5 Hz).

(18) Characteristic ^1H NMR data of **3**: $J_{9,14}$ = $J_{8,9}$ = 11.5 Hz, $J_{8,17}$ = 5.3 Hz, $J_{14,15}$ = 1.8 Hz, $J_{14,16}$ = 2.7 Hz, $J_{15,16}$ = 10.0 Hz, $J_{16,17}$ = 5.2 Hz, $J_{15,17}$ = 1.2 Hz, $J_{13,14} \cong 2$ Hz; major *cis*, $J_{9,14}$ = 6.2 Hz; minor *cis*, $J_{9,14}$ = 6.0 Hz.

(19) The narrow $W_{1/2}$ (7 Hz) of the ester carbinol proton (10-H, δ 5.14) of **18** supported the depicted C10 stereochemistry in **17**.

(20) 2(*S*)-Methylbutyric anhydride [bp 65.5 °C (~1 mmHg), $[\alpha]^{24}_D$ +29.2° (neat)] was prepared from 2(*S*)-methylbutanol (Nakarai) by the standard procedures; see ref 5a.

Novel Binuclear Platinum(III) Diphosphite Complexes

Chi-Ming Che,[1a] William P. Schaefer,[1a] Harry B. Gray,*[1a]
Mark K. Dickson,[1b] Paul B. Stein,[1b] and
D. Max Roundhill*[1b]

Contribution No. 6600 from the
Arthur Amos Noyes Laboratory
California Institute of Technology
Pasadena, California 91125
and from the Department of Chemistry
Washington State University
Pullman, Washington 99164

Received February 22, 1982

Relatively few platinum(III) complexes have been reported to date. The best characterized are Pt–Pt-bonded binuclear species, with Pt–Pt distances in the range 2.47–2.56 Å.[2] In recent experiments we have found that binuclear Pt(III) complexes can be generated readily through oxidative addition to a binuclear platinum(II) tetrakis(diphosphite), $Pt_2(pop)_4^{4-}$ (pop = $P_2O_5H_2^{2-}$).[3] The platinum(III) products of halogen and methyl iodide oxidative-addition reactions are described in this communication.

The binuclear Pt(II) species $Pt_2(pop)_4^{4-}$ reacts rapidly with halogens (or CH_3I) to give $Pt_2(pop)_4X_2^{4-}$ (or $Pt_2(pop)_4(CH_3)I^{4-}$).[4] The Pt–Pt distance in $Pt_2(pop)_4Cl_2^{4-}$ (Figure 1)[5] is 2.695 (1) Å,

---

(1) (a) California Institute of Technology; (b) Washington State University.

(2) (a) $K_2[Pt_2(SO_4)_4(H_2O)_2]$, Pt–Pt = 2.47 Å: Muravieskaya, G. S.; Kukina, G. A.; Orlova, V. S.; Evstefera, O. N.; Porai-Koshits, M. A. *Dokl. Akad. Nauk. SSSR* **1976**, *226*, 596–599. (b) $Pt_2(O_2C_2F_3)_2(CH_3)_4(NC_6H_7)_2$, Pt–Pt = 2.557 Å: Schagen, J. D.; Overbeck, A. R.; Schenk, H. *Inorg. Chem.* **1978**, *17*, 1938–1940. (c) $Pt_2(C_5H_4NO)_2(NH_3)_4(NO_3)_2$, Pt–Pt = 2.539 (1) Å: Hollis, L. S.; Lippard, S. J. *J. Am. Chem. Soc.* **1981**, *103*, 6761–6763. (d) $Na_2[Pt_2(HPO_4)_4(H_2O)_2]$, Pt–Pt = 2.486 (2) Å: Cotton, F. A.; Falvello, L. R.; Han, S. *Inorg. Chem.* **1982**, *21*, 1709–1710.

(3) Striking luminescence led to the discovery of the platinum anion (Sperline, R. P.; Dickson, M. K.; Roundhill, D. M. *J. Chem. Soc., Chem. Commun.* **1977**, 62–63), and the emission intensity linearity has been used for the spectrophotometric detection of trace platinum (Dickson, M. K.; Peltee, S. K.; Roundhill, D. M. *Anal. Chem.* **1981**, *53*, 2159–2160. The compound $K_4[Pt_2(pop)_4]\cdot 2H_2O$ has been structurally characterized (Filomena Dos Remedios Pinto, M. A. Sadler, P. J.; Neidle, S.; Sanderson, M. R.; Subbiah, A. *J. Chem. Soc., Chem. Commun.* **1980**, 13–15).

(4) $K_4[Pt_2(pop)_4X_2]$ (X = Cl, Br) was prepared by adding excess X_2 and then KX to an aqueous solution of $K_4[Pt_2(pop)_4]\cdot 2H_2O$ at room temperature. $[Ph_4As]_4[Pt_2(pop)_4I_2]$ was prepared by adding excess I_2 to $[Ph_4As]_4[Pt_2(pop)_4]$ in acetonitrile solution. Anal. Calcd for $K_4[Pt_2(pop)_4Cl_2]\cdot 2H_2O$: P, 20.2; Cl, 5.77. Found: P, 19.0; Cl, 6.17. Anal. Calcd for $K_4[Pt_2(pop)_4Br_2]$: P, 19.3; Br, 12.5. Found: P, 19.2; Br, 12.4. Anal. Calcd for $[Ph_4As]_4[Pt_2(pop)_4I_2]$: P, 9.00; I, 9.22. Found: P, 9.80; I, 9.22. Anal. Calcd. for $K_4[Pt_2(pop)_4(CH_3)I]$: C, 0.95; H, 0.88; I, 10.0; P, 19.6. Found: C, 1.25; H, 0.78; I, 10.5; P, 19.4. The complexes are diamagnetic 1:4 electrolytes and are very stable both in the solid state and in solution.

0002-7863/82/1504-4253$01.25/0

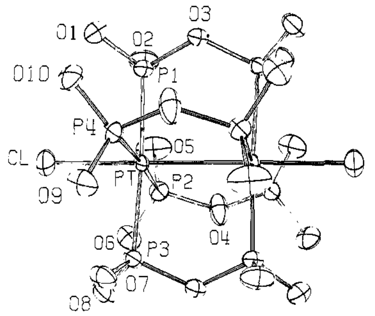

Figure 1. ORTEP drawing of the structure of $Pt_2(pop)_4Cl_2^{4-}$.

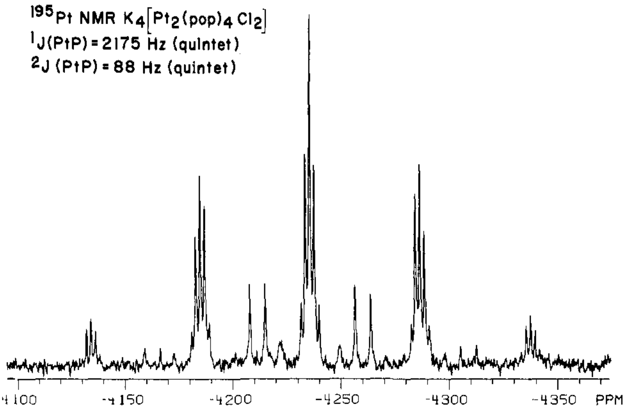

Figure 2. ^{195}Pt NMR spectrum of $K_4[Pt_2(pop)_4Cl_2]$ in aqueous solution at 25 °C.

which is considerably shorter than that (2.925 (1) Å) found for $K_4[Pt_2(pop)_4]\cdot 2H_2O$.[3] The P–O distances are typical of phosphites and pyrophosphites. The Pt–P and Pt–Cl distances are 2.350 (2) and 2.407 (2) Å, respectively. The latter is slightly longer than Pt–Cl in *cis*-$[Pt(NH_3)_2Cl_2]$ (2.33 (1) Å)[6] or $PtCl_4^{2-}$ (2.33 (5) Å).[7]

The ^{31}P NMR spectra of $Pt_2(pop)_4X_2^{4-}$ exhibit single resonances (δ 27.96 (Cl), 24.01 (Br), 18.01 (I)). The satellites attributable to $Pt^{195}Pt(pop)_4X_2^{4-}$ have the following ^1J(PtP) values: ca. 2085 (Cl), 2100 (Br), and 2148 Hz (I). Additional lines in the spectrum of $Pt_2(pop)_4Cl_2^{4-}$ are due to $^{195}Pt^{195}Pt(pop)_4Cl_2^{4-}$. The ^{195}Pt NMR spectra of $Pt_2(pop)_4X_2^{4-}$ exhibit resonances centered at δ −4236 (Cl) (Figure 2), −4544 (Br), and −5103 (I). The satellites are quintets attributable to ^1J(PtP) and ^2J(PtP) (the extra lines are assigned to 11% $^{195}Pt^{195}Pt$). Simple first-order analysis gives the following: ^1J(PtP), 2175 (Cl), 2183 (Br), 2202 Hz (I); ^2J(PtP), 88 (Cl), 82 (Br), 75 Hz (I).[8] The ^2J(PtP) coupling shows that the binuclear structure is retained in solution, and the quintet splitting pattern confirms that the halides occupy axial positions.

The ^{1}H NMR spectrum of the CH_3I adduct[9] shows a quintet (δ 1.51 (^3J(PH) = 5.24 Hz)) flanked by two sets of ^{195}Pt satellites (^2J(PtH) = 52.66 Hz, ^3J(PtH) = 13.83 Hz). Superposed on these 25 lines are 20 lines attributable to $^{195}Pt^{195}Pt(pop)_4(CH_3)I^{4-}$. The ^{13}C NMR decoupled spectrum[10] (^1J(PtC) = 377 Hz, ^2J(PtC) = 134 Hz) is a doublet of doublets attributable to $^{195}Pt^{195}Pt(pop)_4(CH_3)I^{4-}$. The 1-hydrogen-coupled ^{13}C NMR spectrum shows the expected quartet with ^1J(CH) = 142.27 Hz (Figure 3). The ^{31}P NMR spectrum shows a complex second-order pattern with resonances centered at δ 32.68 (^1J(PtP) = 2274 Hz) and 30.32 (^1J(PtP) = 2454 Hz); the ^{195}Pt spectrum has resonances at δ −4311 (^1J(PtP) = 2274 Hz, ^2J(PtP) = 45.5 Hz) and −5227 (^1J(PtP) = 2454 Hz, ^2J(PtP) = 85.7 Hz). These data confirm that the complex is binuclear with the CH_3 and I ligands in axial positions.

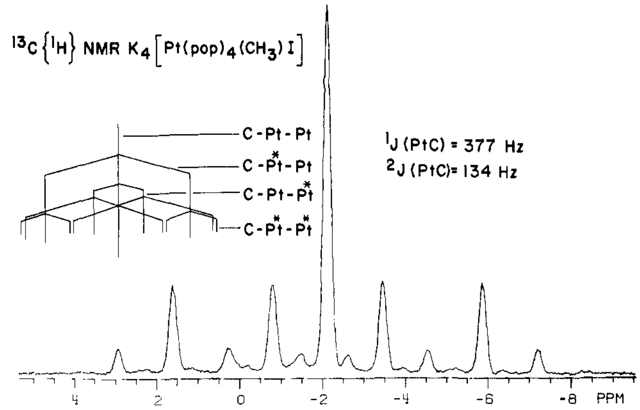

Figure 3. $^{13}C[^1H]$ NMR spectrum of $K_4[Pt_2(pop)_4(CH_3)I]$ in aqueous solution at 25 °C.

Formation of a Pt–Pt single bond apparently drives these binuclear oxidative-addition reactions. Simple theory predicts that two Pt–Pt dσ^* electrons are transferred to X_2 in each product complex ($[Pt(II)]_2$ is $(d\sigma)^2(d\sigma^*)^2$; $[Pt(III)]_2$ is $(d\sigma)^2$),[11-13] which accords with the observed Pt–Pt bond shortening in $Pt_2(pop)_4Cl_2^{4-}$. Furthermore, the intense two-band pattern attributable to a $(d\sigma)^2$ ground state (the higher energy, relatively more intense component is assigned to $d\sigma \rightarrow d\sigma^*$)[11] is observed in the electronic absorption spectrum of each complex (X = Cl, 345 (ϵ 8190), 282 (ϵ 48 840); Br, 340 (ϵ 11 780), 305 (ϵ 55 420); I, 435 (ϵ 15 930), 338 nm (ϵ 42 930)) in aqueous solution.[14] Finally, symmetrical stretching frequencies (Pt–Pt and Pt–X) were obtained from resonance Raman spectral measurements on $K_4[Pt(pop)_4X_2]$ (X = Cl, Pt–Pt = 158, Pt–Cl = 304; Br, Pt–Pt = 134, Pt–Br = 222; I, Pt–Pt = 110, Pt–I = 195 cm^{-1}) in aqueous solution. Increased mixing of halide character according to I > Br > Cl in the dσ (Pt–Pt) wave function is evident from the trends established in both E ($d\sigma \rightarrow d\sigma^*$) and $\bar{\nu}$ (Pt–Pt) (Cl > Br > I). Both UV and resonance Raman spectroscopic indicators (along with the relatively short Pt–Pt distance in the case of $Pt_2(pop)_4Cl_2^{4-}$) suggest that the Pt–Pt single bond in $Pt_2(pop)_4X_2^{4-}$ is even stronger than Rh–Rh in $Rh_2b_4X_2^{2+}$ complexes.[15] The implication is that oxidative addition to binuclear Pt(II) is unusually favorable energetically, which is a feature that we hope to exploit in substrate-activation studies now in progress.

Acknowledgment. Research at the California Institute of Technology was supported by National Science Foundation Grant CHE78-10530. Research at Washington State University was

---

(5) $K_4[Pt_2(pop)_4Cl_2]\cdot 2H_2O$, mol. wt. 1229.37, triclinic, $P\bar{1}$, a = 9.426 (2) Å, b = 9.534 (1) Å, c = 8.743 (1) Å, α = 99.07 (1)°, β = 101.66 (1)°, γ = 118.94 (1)°, Z = 1, ρ_c = 3.18 (1) g cm^{-3}, $F(000)$ = 574, λ(Mo Kα) = 0.71 069 Å, μ = 128.8 cm^{-1}. The crystal was 0.12 × 0.17 × 0.29 mm. 2981 reflections were measured on a Syntex $P2_1$ with graphite-monochromatized Mo Kα radiation and corrected for Lp factor and absorption. The structure was solved by Patterson and Fourier methods and refined by using all data by least squares to an R index of 0.038 ($R = \sum |F_o - |F_c|| / \sum F_o$ for $F_o^2 > 0$). All heavy atoms were refined anisotropically. Hydrogen atoms were not located, but it seems preferable to assume that they are between O(7) and O(9), for example, rather than O(9) and O(10).

(6) Milburn, G. H. W.; Truter, M. R. *J. Chem. Soc. A* **1966**, 1609–1616.

(7) Dickinson, R. G. *J. Am. Chem. Soc.* **1922**, *44*, 2404–2411.

(8) NMR data are reported with positive high-frequency ppm shifts. ^{31}P spectra are referenced to 85% H_3PO_4 and ^{195}Pt spectra to H_2PtCl_6: Kerrison, S. J. S.; Sadler, P. J. *J. Magn. Reson.* **1978** *31*, 321–325.

(9) The infrared spectrum of $K_4[Pt_2(pop)_4(CH_3)I]$ (KBr pellet) exhibits $\bar{\nu}$ (CH) at 2920 cm^{-1} and a CH_3 deformation at 1220 cm^{-1}.

(10) The adduct for this experiment was prepared from 90% enriched $^{13}CH_3I$.

(11) Lewis, N. S.; Mann, K. R.; Gordon, J. G., II; Gray, H. B. *J. Am. Chem. Soc.* **1976**, *98*, 7461–7463.

(12) (a) Rice, S. F.; Gray, H. B. *J. Am. Chem. Soc.* **1981**, *103*, 1593–1595. (b) Dallinger, R. F.; Miskowski, V. M.; Gray, H. B.; Woodruff, W. H. *Ibid.* **1981**, *103*, 1595–1596. (c) Rice, S. F.; Gray, H. B., to be submitted for publication.

(13) (a) Fordyce, W. A.; Brummer, J. G.; Crosby, G. A. *J. Am. Chem. Soc.* **1981**, *103*, 7061–7064. (b) Che, C.-M.; Butler, L. G.; Gray, H. B. *Ibid.* **1981**, *103*, 7796–7797.

(14) The spectrum of $[Ph_4As]_4[Pt_2(pop)_4I_2]$ was measured in acetonitrile solution at 25 °C.

(15) For example, parameters for $Rh_2b_4Cl_2^{2+}$ (b = 1,3-diisocyanopropane) are as follows: Rh–Rh, 2.837 (1) Å (Mann, K. R.; Bell, R. A.; Gray, H. B. *Inorg. Chem.* **1979**, *18*, 2671–2673); E ($d\sigma \rightarrow d\sigma^*$), 338 nm (Mann, K. R.; Lewis, N. S.; Miskowski, V. M.; Erwin, D. K.; Hammond, G. S.; Gray, H. B. *J. Am. Chem. Soc.* **1977**, *99*, 5525–5526); $\bar{\nu}$(Rh–Rh), 134 cm^{-1} (Smith, T. P.; Miskowski, V. M.; Gray, H. B., to be submitted for publication).

supported by the donors of the Petroleum Research Fund, administered by the American Chemical Society. We thank D. Appel and G. Andrews for assistance with the NMR experiments (the NMR equipment was acquired through grants from NSF (CHE79-09984 to the University of Idaho) and the Boeing Company (WSU)).

Registry No. $K_4[Pt_2(pop)_4Cl_2]\cdot 2H_2O$, 82135-56-6; $K_4[Pt_2(pop)_4Br_2]$, 82135-55-5; $[Ph_4As]_4[Pt_2(pop)_4I_2]$, 82135-54-4; $K_4[Pt_2(pop)_4(CH_3)I]$, 82135-52-2; $K_4[Pt_2(pop)_4]$, 82135-51-1; $[Ph_4As]_4[Pt_2(pop)_4]$, 82149-95-9.

Novel Nickel(II) Complexes with Doubly Deprotonated Dioxopentaamine Macrocyclic Ligands for Uptake and Activation of Molecular Oxygen

Eiichi Kimura,* Atsuko Sakonaka, and Ryosuke Machida

Department of Medicinal Chemistry, Hiroshima University
School of Medicine, Kasumi, Hiroshima 734, Japan

Mutsuo Kodama

Department of Chemistry, College of General Education
Hirosaki University, Bunkyo, Hirosaki 036, Japan

Received October 5, 1981

The chemical interest in interaction and activation (by reduction) of molecular oxygen by copper proteins has grown considerably during recent years.[1] Copper(II)[2,3] and nickel(II)[4,5] can promote the reactions between O_2 and peptides, where Cu(III) and Ni(III) peptide complexes were considered as intermediates. Cu(III) and Ni(III) ions have been obtained with complexes of peptides (such as L^4)[6-8] and macrocyclic polyamines such as L^3 or L^6.[9-13] Very recently, we have shown that dioxotetraamine macrocycles (e.g., L^5) possess dual characters of macrocyclic tetraamines (e.g., L^6) and of tripeptide L^4 to form square-planar complexes $[MH_{-2}L]^0$, **1**,[14,15] and tend to lower the redox potentials E^0 for M(II) ⇌ M(III) couples.[16] However, the E^0 values so far reported in our models were not low enough to make M(III) states readily accessible in biological conditions (e.g., air-oxidation).

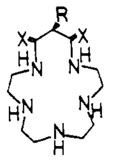

L^1, X = O; R = H
L^2, X = O; R = $CH_2C_6H_5$
L^3, X = H_2; R = H

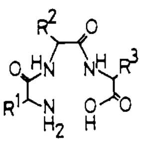

L^4
(tripeptides)

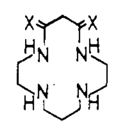

L^5, X = O
L^6, X = H_2

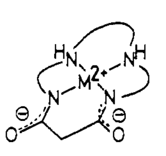

1

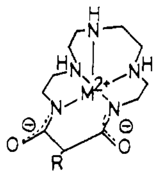

2

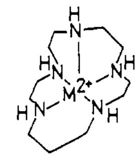

3

In developing a closer mimic to redox enzymes, we have synthesized new ligands, the dioxopentaamine macrocycles L^1 and L^2.[17] Herein we communicate that *the special steric and electronic effects imposed by the basal two imide anions and an axial N donor of the pentaamine macrocyclic ligands in the rigid square-pyramidal structure* **2** *facilitate the generation of nickel(III) ion and further permit the formation of hitherto unknown 1:1 Ni–O_2 adducts at room temperature in air oxidation. Moreover, the benzyl substituent in L^2 effects a reversible Ni–O_2 interaction.* We have also discovered that *dioxygen is activated by coordinating with the nickel(II) complexes so as to convert benzene into phenol.*

The 1:1 M(II)–L^1 pH metric titrations in N_2 atmosphere and their analysis (as for L^5)[14] established formation of the doubly deprotonated complexes $[M(H_{-2}L)]^0$ above pH 9: $K_{MH_{-2}L}$ (= $[MH_{-2}L][H^+]^2/[M][L]$) = 2.6×10^{-9} M for Ni(II) and 9.3×10^{-3} M for Cu(II) at 25 °C and *I* 0.2 M. In contrast to the yellow Ni(II)–L^5 and –L^6 complexes,[16] the pink Ni(II)–L^1, –L^2, and –L^3 show d–d absorption spectral patterns (see Figure 1) indicative of octahedral high-spin species, to lend a support to the square-pyramidal structures **2** and **3**.[18] The conjugated two imide anions of L^1 and L^2 should lie at the basal part of the square-pyramidal ring, which may add rigidity and constriction to the in-plane N_4 ligand field of L^3, as illustrated by the higher intensities of d–d transitions for L^1 and L^2 complexes than for the L^3 complex with Ni(II).

Cyclic voltammetry was used to determine the redox potentials E^0 for M(II) ⇌ M(III) in L^1, L^2, L^3 complexes.[19] An interesting result with L^1 and L^2 (Table I) is that the $Ni^{III,II}$ potentials are much smaller than the corresponding $Cu^{III,II}$ potentials, reflecting coordinate environments much more favorable for the d^8 Ni(II) → d^7 Ni(III) transition than for the d^9 Cu(II) → d^8 Cu(III). A more remarkable fact is that the E^0 values of Ni (+0.24 V *vs.* SCE) are the lowest of all the reported $M^{III,II}$ values for the relevant polyamines (inclusive of the dioxo-free counterpart L^3 complex)[11,12,16] and oligopeptides.[5-8,20]

The dark brown developed as the pink solution (unbuffered, initial pH 10.1) of Ni(II)–L^1 and –L^2 complexes were oxidized electrochemically (final pH 7.1). The UV–visible spectra of the oxidation products (λ_{max} 300 nm, ϵ 6900 M^{-1} cm^{-1} for L^1 and λ_{max} 270 nm, ϵ 7400 M^{-1} cm^{-1} for L^2 (see Figure 1c)) are indicative

---

(1) "Bioinorganic Chemistry. II"; K. N. Raymond, Ed.; American Chemical Society: Washington, D.C., 1977; Adv. Chem. Ser. No. **162**, pp 127–349.

(2) Burce, G. L.; Paniago, E. B.; Margerum, D. W. *J. Chem. Soc., Chem. Commun.* **1975**, 261.

(3) Kurtz, J. L.; Burce, G. L.; Margerum, D. W. *Inorg. Chem.* **1978**, *17*, 2454.

(4) Paniago, E. B.; Weatherburn, D. C.; Margerum, D. W. *J. Chem. Soc., Chem. Commun.* **1971**, 1428.

(5) Bossu, F. P.; Paniago, E. B.; Margerum, D. W.; Kirksey, S. T., Jr.; Kurtz, J. L. *Inorg. Chem.* **1978**, *17*, 1034.

(6) Bossu, F. P.; Chellappa, K. L.; Margerum D. W. *J. Am. Chem. Soc.* **1977**, *99*, 2195.

(7) Margerum, D. W.; Wong, L. F.; Bossu, F. P.; Chellappa, K. L.; Czarnecki, J. J.; Kirksey, S. T., Jr.; Neubecker, T. A., ref 1, p 281.

(8) Bossu, F. P.; Margerum, D. W. *Inorg. Chem.* **1977**, *16*, 1210.

(9) Barefield, E. K.; Lovecchio, F.; Tokel, N. E.; Ochiai, E.; Busch, D. H. *Inorg. Chem.* **1972**, *11*, 283.

(10) Lovecchio, F. V.; Gore, E. S.; Busch, D. H. *J. Am. Chem. Soc.* **1974**, *96*, 3109.

(11) Fabbrizzi, L. *J. Chem. Soc. Chem. Commun.* **1979**, 1063.

(12) Zeigerson, E.; Ginzburg, G.; Schwartz, N.; Luz, Z.; Meyerstein, D. *J. Chem. Soc., Chem. Commun.* **1979**, 241.

(13) Zeigerson, E.; Ginzburg, G.; Meyerstein, D.; Kirschenbaum, L. J. *J. Chem. Soc., Dalton Trans.* **1980**, 1243.

(14) Kodama, M.; Kimura, E. *J. Chem. Soc., Dalton Trans.* **1979**, 325.

(15) Kodama, M.; Kimura, E. *J. Chem. Soc., Dalton Trans.* **1979**, 1783.

(16) Kodama, M.; Kimura, E. *J. Chem. Soc., Dalton Trans.* **1981**, 694.

(17) Synthesized from tetraethylenepentaamine and diethyl malonate in refluxing ethanol for a week. Both L^1 (mp 174 °C) and L^2 (mp 194 °C) gave satisfactory elemental analysis and NMR data.

(18) The high-spin Ni(II) complex of the N_5-donor L^1 is less stable than the low-spin complex of the N_4-donor L^5 ($K_{MH_{-2}L} = 7.0 \times 10^{-6}$ M^{-1})[16] at a given pH. In parallel, Ni^{II}–L^3 ($K_{ML} = 5.2 \times 10^{17}$ M^{-1}) is less stable than Ni^{II}–L^6 ($K_{ML} = 5 \times 10^{22}$ M^{-1}).

(19) The voltammograms show quasi-reversible behavior by similar criteria (the separation of the anodic and cathodic peaks by E = ca. 80 mV and peak current ratios nearly unity, etc.) applied to those for Ni^{II}–L^4 and –L^5 complexes.[16]

(20) Much more negative potentials for the Ni^{2+}/Ni^{3+} couple in organic solvents were previously reported with planar macrocycle tetraamine ligands having dianionic, charge-delocalized chelate rings. However, their O_2 adducts formtion was not mentioned: Pillsburg, D. G.; Busch, D. H. *J. Am. Chem. Soc.* **1976**, *98*, 7836. Streeky, J. A.; Pillsbury, D. G.; Bush, D. H. *Inorg. Chem.* **1980**, *19*, 3148.

0002-7863/82/1504-4255$01.25/0